Green synthesis of bioactive oligopeptides promoted by recyclable nanocrystalline hydroxyapatite

Green synthesis of bioactive oligopeptides promoted by recyclable nanocrystalline hydroxyapatite

Michele Anselmi†,1, Pasquale Stavole†,1, Elisa Boanini1, Adriana Bigi1, Eusebio Juaristi2 &

Luca Gentilucci*,1

1 Department of Chemistry “Giacomo Ciamician”, University of Bologna, via Selmi 2, 40126 Bologna, Italy

2 Center for Research & Advanced Studies of the National Polytechnic Institute (Cinvestav), Av. Instituto Polite´ cnico Nacional 2508,

San Pedro Zacatenco, Gustavo A. Madero, 07360 Mexico City, CDMX, Mexico

*Author for correspondence: Tel.: +39 051 209 9570; Fax: +39 051 209 9456; luca.gentilucci@unibo.it

† Authors contributed equally

Aim: The pharmaceutical industry is showing renewed interest in therapeutic peptides. Unfortunately, the chemical synthesis of peptides remains very expensive and problematic in terms of environmental sustainability. Hence, making peptides ‘greener’ has become a new front line for the expansion of peptide market. **Results:** We developed a mechanochemical solvent-free peptide bond-forming protocol using standard reagents and nanocrystalline hydroxyapatite as a bio-compatible, reusable inorganic base. The reaction was also conducted under ultra-mild, minimal solvent-grinding conditions, using common laboratory equipment. **Conclusion:** The efficacy of the described protocol was validated with the convenient preparation of endomorphin-1, H-Tyr-Pro-Trp-Phe-NH2, the endogenous ligand of the μ-opioid receptor, currently regarded as a lead for the discovery of painkillers devoid of harmful side effects.

Graphical abstract:

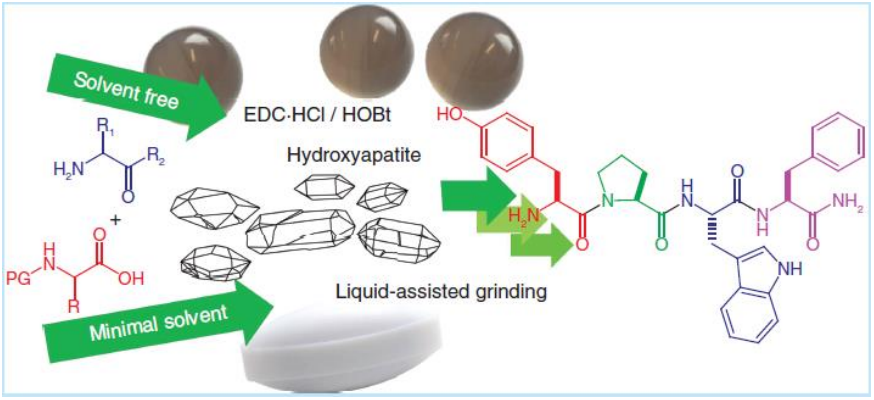

Keywords: ball-milling · bioactive peptide · endomorphin-1 · green synthesis · hydroxyapatite · mechanochemistry · opioid peptide · recyclable base · solvent-free

Despite their tremendous potential [1], for long time bioactive peptide drugs have been considered as a specialists’ niche area [2]. The reason for this reputation largely stems from their limited *in vivo* stability and rather low to null bioavailability. These limitations can be for the most part circumvented by the ‘peptidomimetic’ approach, in other words, by introducing properly designed structural modifications in the active peptide [3]. Otherwise, one may consider the adoption of alternative routes of administration, for example subcutaneous, nasal, pulmonary

and others [2]. Consequently, in the past few years, there has been renewed interest in the development of more effective therapeutic peptides, in particular for the treatment of metabolic diseases (e.g., liraglutide), autoimmune diseases (e.g., glatiramer) and in oncology (e.g., octreotide) [2].

Yet, the accessibility to many peptidic drugs is still hampered by their expensive production and challenging purification [4]. While sizeable peptides and proteins can be obtained by recombinant technologies, short and medium size peptides are usually prepared by chemical synthesis, being the recourse to enzymatic synthesis more limited [5]. Unfortunately, the solid-phase synthesis of peptides (SPPS) on insoluble polymeric supports makes use of a large excess of amino acids and of coupling agents. On the other hand, in-solution synthesis of medium size peptides requires tedious isolation steps. Furthermore, both SPPS and solution synthetic methods require extensive protection/deprotection strategies. Finally, each coupling/deprotection cycle generally makes use of large volumes of hazardous organic solvents, such as dichloromethane (DCM), dimethylformamide (DMF),*N*-methylpyrrolidone or methanol, producing a huge amount of wastes [6]. As a consequence, the chemical preparation of peptides is among the most problematic synthetic procedures in terms of atom economy and environmental sustainability [6,7].

One opportunity for making peptide synthesis more sustainable [8] consists in the use of nontoxic reagents, for example by the replacement of standard organic solvents with green alternatives [9–11]. In this context, some protocols have been developed to perform amino acid coupling in an aqueous environment [12–15]. A complementary alternative is the drastic reduction of the involved volumes of solvent used [16,17]. Coupling reactions can be performed under ball-milling mechanochemical [18–22], or mechanoenzymatic [23,24], solvent-free conditions. To improve the homogeneity of the solid-state reactions, minimal amounts of solvents can be added (liquid-assisted grinding, LAG), resulting in increased yields and shorter reaction times [19,25,26]. Finally, toxic bases such as trimethylamine, *i*Pr2NEt or lutidine, typically utilized in peptide synthesis, can be replaced by inorganic salts, for example, NaHCO3 [18,25] or hydrotalcite [19,27].

In this context, we turned our attention to hydroxyapatite (HAp), Ca10(PO4)6(OH)2, as a convenient inorganic base for potential activation of peptide synthesis. HAp, one of the most usual forms of calcium phosphate, is highly biocompatible thanks to its chemical and structural similarity to the mineral phase of bone tissues. In this regard, synthetic HAp differs from natural apatites, which display much lower crystallinity and poor stoichiometry. HAp powders can be synthesized following different procedures, in other words, by means of direct synthesis in aqueous solution, under microwave or ultrasound irradiation, through mechanochemical, hydrothermal, sol-gel, as well as phase transition methods [28,29]. The properties of HAp vary depending on the method of preparation, thus enabling their use as nanomaterials [30], and for diverse applications in the biomedical field [31], including bone tissue engineering [32,33], drug controlled release [34], imaging [35], as well as in heterogeneous catalysis (cross-couplings,

condensations, oxidations, photocatalysis etc.) [36,37].

The structure of hexagonal HAp, space group *P*63*/m*, shows a compact assembly of tetrahedral PO4 groups, and two crystallographically independent cation sites, Ca(I) and Ca(II). The four Ca(I) are strictly aligned in columns parallel to the crystallographic *c*-axis, whereas the six Ca(II) are positioned at the apexes of staggered equilateral triangles. These triangles form the walls of channels parallel to the *c*-axis and filled by the OH- ions. Thus, HAp displays an 'open' and flexible structure that tolerates a large number of anionic and cationic substitutions. Potential

Lewis basic sites, such as PO4 3- and OH- groups, together with Ca2+ Lewis acid sites and POH Brønsted acid sites, have been recognized on the surface of HAp [38–40].

The use of HAp as a base may offer numerous advantages in peptide synthesis, due to its low solubility, high thermal stability and relatively weak basic character that may prevent side reactions promoted by the support itself.

Moreover, HAp displays a great affinity for amino acids, especially in the carboxylate form which interacts with the

exposed Ca2+ ions [41].

Herein, we present an expedient solvent-free peptide bond formation between *N*-protected amino acids and amino ester*/*amide · HCl salts counterparts, using a ball-mill and the standard *N*-(3-dimethylaminopropyl)-*N*_-ethylcarbodiimide · hydrochloride*/*hydroxybenzotriazole (EDC · HCl*/*HOBt) coupling agents, in the presence of nanocrystalline HAp as a bio-compatible base that can be reused without substantial loss of efficacy after easy regeneration. *N*-(3-Dimethylaminopropyl)-*N*_-ethylcarbodiimide · hydrochloride (EDC · HCl) is among the most utilized coupling agents for in-solution peptide synthesis, since the resulting urea by-product is easily removed from

the reaction mixture by washing with acidic aqueous solutions. Besides, EDC · HCl has proved to be very efficient in

solvent-free reactions. EDC · HCl exists exclusively in cyclic form, and easily undergoes transformation to a pseudo

cyclic stable intermediate in reaction with carboxylic acids forming a low-melting phase [42]. We also report the optimization of the LAG reactions under very mild conditions, in other words, in a standard glass round bottom flask equipped with a common polytetrafluoroethylene-coated magnetic stirring bar.

Materials & methods

General methods

All commercially available reagents purchased from Merck (Darmstadt, Germany) were used without further purification. Ballmilling was carried out in a PlanetaryMill Pulverisette (Fritsch GmbH, Idar-Oberstein,Germany), mounting an agate jar (ø = 7.5 cm) equipped with three balls of the same material (ø = 2.0 cm). Purities were assessed by analytical reverse phase high-performance liquid chromatography (RP-HPLC) on a 1100 series apparatus

(Agilent, CA, USA), using a reverse phase (RP) column mod. Gemini (Phenomenex, Castel Maggiore, Italy) 3 μ C18 110 °A 100 × 3.0 mm (particle size 3 μm, pore size 110 ° A, length 100 mm, internal diameter 3 mm); DAD 210 nm; mobile phase: from 9:1 solvent A*/*solvent B to 2:8 solvent A*/*solvent B, in 8 min, at a flow rate of 0.8 ml min-1, followed by 10 min at the same composition; for the analysis of crude reaction mixtures, A = 0.5% HCOOH in H2O, B = 0.5% HCOOH in CH3CN; for the analyses of the mixtures after work-up, A = H2O

and B = CH3CN. ESI-MS was done on a MS single quadrupole HP 1100 MSD detector (Agilent). 1H NMR was performed at 400 MHz on a Varian Gemini 400 (Agilent) in 5 mm tubes in CDCl3 at room temperature (rt); chemical shifts are reported as δ values relative to residual CHCl3 (δH = 7.26 ppm).

HAp nanocrystals

The procedure was performed under N2 atmosphere and using CO2-free distilled water. The synthesis of HAp was carried out using 50 ml of 0.65 M (NH4)2HPO4 solution at pH adjusted to ten with NH4OH. The solution was heated to 90◦C and 50 ml of 1.08 M Ca(NO3)2・4H2O solution, pH 10 adjusted with NH4OH was added dropwise under stirring. The resulting suspension was stirred for 5 h at 90◦C, the precipitate that formed was isolated by centrifugation at 10,000 rpm, and repeatedly washed with CO2-free distilled water. The product was dried at 37◦C overnight.

Fourier transform IR (FTIR) analysis was done on a Alpha FTIR spectrophotometer (Bruker, MA, USA); 1 mg of the powdered HAp was mixed with 300 mg of KBr (infrared grade) and pelletized at the pressure of 10 tons in 2 min. The pellets were analyzed in the range 4000–500 cm-1, 32 scans, resolution 4 cm-1.

Powder x-ray diffraction patterns were recorded using a PANalytical-X'Pert PRO powder diffractometer (Malvern Panalytical-Spectris, Egham, UK) equipped with a fast X'Celerator (Malvern Panalytical-Spectris) detector (λ = 0.154 nm, 40 mA, 40 kV). For phase identification, the 2θ range was investigated from 10 to 60 2θ ◦ with a step size of 0.1◦ and time/step of 100 s. For evaluation of cell parameters, x-ray powder data were collected with a fixed counting time of 400 s for each 0.033/step. The Rietveld routine of the HighScore Plus software package (Malvern Panalytical-Spectris) was used to process data.

For transmission electron microscopy (TEM) investigations, a small amount of powder was dispersed in ethanol and submitted to ultra-sonication. A drop of the calcium phosphate suspension was transferred onto holey carbon foils supported on conventional copper microgrids. A CM 100 transmission electron microscope (Philips, Amsterdam, The Netherlands) operating at 80 kV was used.

Ca and P contents in HAp were measured by means of an inductively coupled plasma spectrometer (ICP-AES, Horiba Jobin Yvon, Kyoto, Japan). Sample was prepared by dissolving 20 mg of powder in 70% nitric acid solution (4 ml) and diluting to final volume of 100 ml.

Zeta potential was measured using electrophoretic light scattering (ZetasizerNano; Malvern Instruments, Malvern, UK). A total of 5 mg of HAp was suspended in 50 ml of MilliQ water after sonication for 2 min. The analysis was performed in triplicate.

The surface area was measured using a Sorpty 1750 BET analyzer (Carlo Erba, Cornaredo, Italy) using constant volume N2 absorption with desorption at 80◦C.

Solvent-free milling

The general procedure is as follows: a mixture of the *N*-protected-amino acid (0.23 mmol), EDC・HCl/HOBt (0.25mmol each) andHAp (50mg) was grinded in an agate jar equipped with three balls of the same material, at the

speed of 8–10 Hz, at room temperature (rt) for 10 min. Then the amino ester/amide counterpart (0.23 mmol) was

added at rt, and the mixture was grinded for 1 h under the same conditions. The mechanical milling was interrupted,

the waxy residue was diluted with EtOH (10 ml), and HAp was recovered by centrifugation (10,000 rpm). The

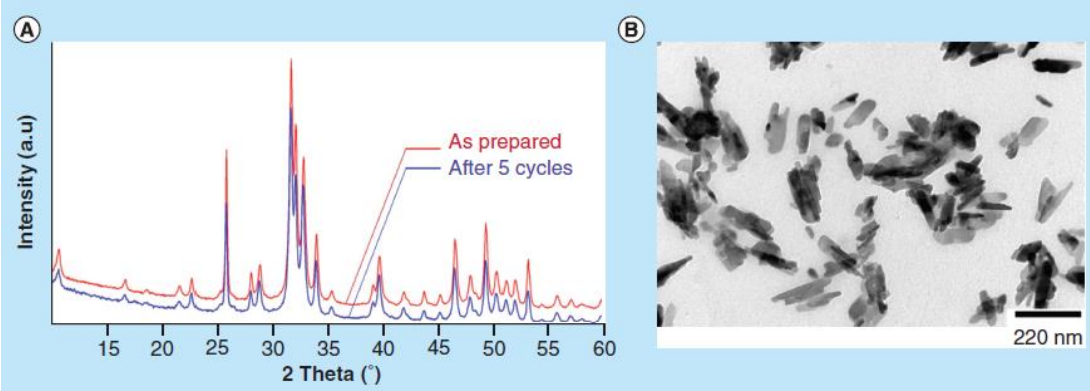

Figure 1. Characterization of hydroxyapatite nanocrystals. (A) Powder x-ray diffraction patterns of hydroxyapatite samples prior to (red) and after (blue) five cycles of peptide bond formation. **(B)** Transmission electron microscopy image of hydroxyapatite nanocrystals; bar = 220 nm.

precipitated crystals were washed with EtOH and centrifuged once more, and stored overnight at 40◦C prior to reuse. The collected supernatant from centrifuged samples were combined and concentrated at reduced pressure,

the residue was diluted with EtOAc (30 ml), and the organic layer was washed in sequence with 1 M HCl, sat. Na2CO3 and brine (5 ml each).

N-Boc solvent-free removal [25]; the protected peptides were placed on a Gooch filter inside a fume hood, and HCl gas was blown through for 3 h. Then the residues were suspended in EtOAc and sonicated for 15 min. The peptide-HCl salts were collected by centrifuge (3000 rpm), and the procedure was repeated.

Minimal solvent-assisted grinding

General procedure: a mixture of the *N*-protected-amino acid (0.23 mmol), EDC · HCl/HOBt (0.25 mmol each), HAp (50 mg) and the solvent (80–200 µl), was grinded in a two-necked glass round bottom flask equipped with an olive-shaped polytetrafluoroethylene-coated stirring bar (*l* = 3.0 cm), under inert atmosphere at rt for 10 min. Then the amino ester/amide counterpart (0.23 mmol) was added at rt, and the mixture was grinded for 2 h under the same conditions. Then the smooth amalgam was diluted with EtOH (10 ml), and HAp was recovered by centrifugation (10,000 rpm). The produced crystals were washed with EtOH and centrifuged once more, and stored overnight at 40◦C prior to reuse. The collected supernatants from centrifuged samples were treated as discussed for the solvent-free ball milling conditions.

Results & discussion

Characterization of HAp

We utilized HAp nanocrystals synthesized by a co-precipitation method. Consistent to the data reported in the literature [31,43,44], the x-ray diffraction pattern of the newly synthesized powder (Figure 1A) showed the presence of

a number of diffraction peaks indicating the presence of HAp (PDF 9-432) as unique crystalline phase. The lattice constants are *a* = 9.421(3) °A and *c* = 6.885(2) ° A. The TEM micrograph (Figure 1B) revealed tiny plate-shaped HAp crystals with mean dimensions of about 100 nm (length) × 30 nm (width). The nanocrystals exhibit a surface

area of 56 m2/g and are negatively charged (zeta potential = -12.5 mV).

The FTIR spectrum (Figure 2A) showed the characteristic absorption bands due to the phosphate groups, in other words, the antisymmetric stretching at 1043 and 1091 cm-1, the symmetric stretching at 962 cm-1 and the bending modes at 601 and 570 cm-1, together with the absorption bands at 3572 and 630 cm-1 due to OHstretching

and bending modes, respectively [31,43,44]. The sharpness of the absorption bands confirmed the good crystallinity of the powder. In agreement, HAp also displayed a good stoichiometry as indicated by the value of the

Ca/P ionic ratio of 1.67.

Initially, this synthetic HAp was employed as a base in a model coupling reaction in solution under standard conditions. *N*-Boc-Val-OH (50 mg, 0.23 mmol) was stirred for 10 min in the presence of the coupling agent EDC · HCl and HOBt as racemization inhibitor (1.2 equiv. each), in 10 ml of 4:1 DCM/DMF and a suspension

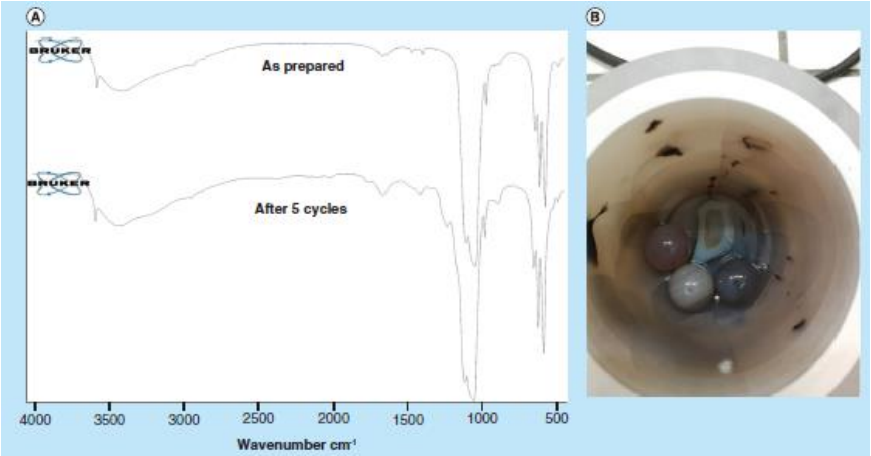

Figure 2. Infrared characterization of hydroxyapatite nanocrystals and solvent-free reaction system. (A) Top, infrared adsorption spectra of fresh hydroxyapatite; bottom, hydroxyapatite after five cycles (pellets in KBr). **(B)** Grinded reaction mixture in an agate jar (ø = 7.5 cm) containing three agate balls (ø = 2.0 cm), at the speed of 8–10 Hz.

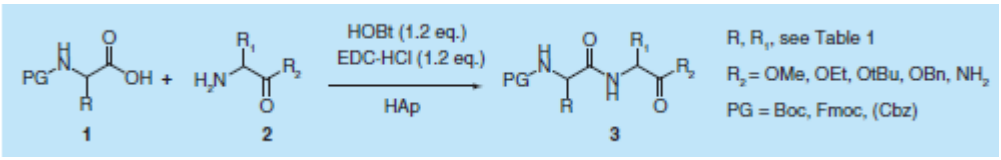

Figure 3. Hydroxyapatite-promoted amide bond formation, general conditions. Boc: Tert-butyloxycarbonyl; Cbz: Benzyloxycarbonyl; EDC · HCl: N-(3-Dimethylaminopropyl)-N_-ethylcarbodiimide · hydrochloride; Fmoc: Fluorenylmethyloxycarbonyl; HAp: Hydroxyapatite; HOBt: Hydroxybenzotriazole; PG: Protecting group.

of HAp (50 mg), under inert atmosphere at rt. H-Phe-OMe · HCl (25 mg, 0.23 mmol) was then added and the resulting mixture was stirred under the same conditions for an additional 4 h (Figure 3).

Following evaporation of the solvent at reduced pressure, the residue was diluted with EtOH and the resulting

solution was centrifuged to recover the HAp powder. The supernatant was separated and concentrated at reduced

pressure, and the residue was diluted with EtOAc and washed in sequence with 1 M HCl, sat. Na2CO3 and brine.

This protocol afforded 65 mg of the crude dipeptide **3a** *N*-Boc-Val-Phe-OMe (72%), as confirmed by the ESI-MS,

in a purity of 80%, as determined by RP-HPLC (58% net yield).

Solvent-free mechanochemistry

Next, peptide coupling reactions were performed under solvent-free conditions, under planetarymilling (Figure 2B)

in an agate jar (ø = 7.5 cm) containing three agate balls (ø = 2.0 cm), at the speed of 8–10 Hz. In order to determine

the scope of the method, the general ball milling procedure was carried out with a variety of amino acids (Table 1).

Mechanical milling was interrupted after 1 h (Figure 2B), and the crude mixture was diluted with EtOH, to

recover HAp by centrifugation. The supernatant was subjected to the same work-up procedure as discussed before.

Gratifyingly, most reactions gave the crude dipeptides in good amount (up to 86%) and high purity (up to

Table 1. Mechanosynthesis of peptides 3 from the *N*-protected amino acids 1 and the amino ester/amide HCl salt partners 2 (0.23 mmol each), after 1 h, in the presence of *N*-ethyl-*N'*-(3-dimethylaminopropyl)carbodiimide·HCl/hydroxybenzotriazole (0.25 mmol each) and hydroxyapatite (25–100 mg).

Entry	1	2·HCl	HAp (mg)	3	Recovered crude mixture (%)†	Purity (%)†,‡	Yield (%)§
1	Boc-Val-OH	H-Phe-OMe	50	a	79	90	71
2	Boc-Val-OH	H-Phe-OMe	100	a	82	90	74
3	Boc-Val-OH	H-Phe-OMe	25	a	68	88	60
4	Boc-Val-OH	H-Phe-OEt	50	b	80	94	75
5	Boc-Val-OH	H-Phe-OEt	46¶	b	78	92	72
6	Boc-Val-OH	H-Phe-OEt	44¶	b	73	94	69
7	Boc-Val-OH	H-Phe-OEt	41¶	b	70	93	65
8	Boc-Val-OH	H-Phe-OEt	38¶	b	68	90	61
9	Boc-Phe-OH	H-Gly-OEt	50	c	75	91	68
10	Boc-Phe-OH	H-D-Val-OMe	50	d	85	93	79
11	Boc-Phe-OH	H-Gly-NH_2	50	e	76	88	67
12	Boc-Phe-OH	H-Leu-OtBu	50	f	72	93	67
13	Boc-Phe-OH	H-D-Ser-OMe	50	g	80#	74#	59
14	Boc-Trp-OH	H-Phe-NH_2	50	h	86	94	81
15	Boc-Tyr-OH	H-Phe-OEt	50	i	73	90	66
16	Boc-Tyr-OH	H-Gly-OEt	50	i	78	85	66
17	Boc-Ser(OBn)-OH	H-Pro-OBn	50	m	70	80	56
18	Fmoc-Phe-OH	H-D-Val-OMe	50	n	65††	87††	57
19	Fmoc-Asp(OtBu)-OH	H-D-Val-OMe	50	o	62††	93††	58
20	Fmoc-Lys(*N*-Cbz)-OH	H-D-Ser-OMe	50	p	55#,††	70#,††	39
21	Fmoc-Lys(*N*-Cbz)-OH	H-Ser-NH_2	50	q	60#,††	73#,††	44

†Determined after aqueous workup.
‡Determined by RP-HPLC.
§Calculated as the recovered crude mixture x purity (%).
¶Recovered from the preceding entry.
#The presence of depsitripeptides was also detected by RP-HPLC and ESI-MS.
††After filtration through a pad of silica gel.
Boc: Tert-butyloxycarbonyl; Cbz: Benzyloxycarbonyl; ESI-MS: Electrospray ionisation mass spectrometry; Fmoc: Fluorenylmethyloxycarbonyl; HAp: Hydroxyapatite; RP-HPLC: Reverse phase high-performance liquid chromatography.

94%; Supplementary Figure 1). The possibility of epimerization in the peptide forming reaction was excluded on the basis of RP-HPLC/ESI-MS and 1HNMRanalyses (Supplementary Figure 2), which is in line with observations reported in the literature [45].

In the coupling between *N*-Boc-Val-OH and H-Phe-OMe · HCl, the yield of **3a** was only slightly improved when the reaction was repeated with increasing amounts of HAp (Table 1, entry 2 vs entry 1), while the reduction of the amount of HAp to 25 mg led to a significant drop of the yield (entry 3 in Table 1).

Recycling of HAp for five cycles

Similar results were obtained for the preparation of dipeptide **3b** from *N*-Boc-Val-OH and H-Phe-OEt · HCl (Table 1, entry 4). Following work-up, the recovered crystalline HAp powder was dried for 8 h at 40 ◦C, and reused in four subsequent cycles of reactions between the same partners (see entries 5–8 in Table 1). After each cycle, the amount of recovered HAp decreased slightly, which might explain the progressive, moderate drop in the amount of crude peptides, from 80 to 68%.

The observed loss of HAp can be attributed to its incomplete recovery after centrifugation, rather than by degradation or solubilization. Indeed, the overall morphology and dimensions of the crystals are preserved after recycling, as shown in the TEM image reported in Supplementary Figure 3. Moreover, x-ray diffraction analysis of the HAp powder isolated from entry 8 showed the same x-ray diffraction patterns as the original material (Figure 1A), supporting that the crystalline structure was preserved. Furthermore, FTIR after five cycles maintained the same profile of the pristine material (Figure 2) without extra peaks, indicating the absence of organic inclusions.

This is in contrast to the behavior of HAp in a wet HCl atmosphere, where both the chemical integrity and particle morphology of HAp are modified. Carbonated domains of HAp appear to facilitate the destabilizing effect of HCl, which results in the elimination of phosphate and OH species and the generation of deep structural groves and voids in the material [45,46].

Amino acids scope

As mentioned above, the generality of the procedure was confirmed by coupling diverse amino acids carrying either the *N*-Boc, *N*-Fmoc or *N*-Cbz protecting groups, with an amino ester (Me, Et, *t*Bu, or Bn) or primary amide partners Figure 3 & Table 1). In general, the *N*-Fmoc protected amino acids gave inferior results (Table 1, entries 18–21) relative to *N*-Boc protected analogs (Table 1, entries 9–17). Furthermore, the usual aqueous work-up procedure failed to efficiently remove the unreacted *N*-Fmoc-amino acids from the crude reaction mixtures. For simplification of the analyses, the unreacted Fmoc-amino acids were removed from the mixtures by filtration through a short pad of silica gel (230–400 mesh) using few ml of 1:1 cyclohexane/EtOAc, affording the crude dipeptides in moderate quantity (55–65%) but acceptable purity (Table 1: entry 18, 87%; entry 19, 95%). In any case, the *N*-Fmoc group proved to be stable during the grinding process; indeed, analysis of the crude reaction mixture did not reveal the presence of the deprotected amino acids, nor condensation products created by their

reaction at the *N*-terminus.

The secondary amine in H-Pro-OBn readily reacted with *N*-Boc-Ser(OBn)-OH (entry 17 in Table 1), affording the anticipated dipeptide **3m** in a good amount (70%) and purity (80%) (Supplementary Figure 4), appearing in the 1H NMR in CDCl3 as a mixture of *cis/*trans rotamers about the Ser-Pro peptide bond (Supplementary Figure 5).

Also amino acids with functionalized side chains have been utilized: H-D-Ser-OMe (entries 13 and 20 in Table 1), *N*-Boc-Trp-OH (entry 14 in Table 1), *N*-Boc-Tyr-OH (entries 15 and 16 in Table 1), *N*-Boc-Ser(OBn)-OH (entry 17 in Table 1), *N*-Fmoc-Asp(O*t*Bu)-OH (entry 19 in Table 1), *N*-Fmoc-Lys(Cbz)-OH (entries 20 and 21 in Table 1) and H-Ser-NH2 (entry 21 in Table 1). Notably, the reaction was tolerant to the unprotected phenol group of Tyr (entries 15 and 16 in Table 1), since analysis of the corresponding reaction mixtures did not show the formation of any depsipeptide. By contrast, the hydroxy group in H-Ser-NH2 and H-D-Ser-OMe gave significant amounts of the following depsitripeptides (as determined by RP-HPLC): entry 13 in Table 1, *N*-Boc-Phe-D-Ser(*N*Boc-Phe)-OMe (22%); entry 20 in Table 1, *N*-Fmoc-Lys(*N*-Cbz)-D-Ser[*N*-Fmoc-Lys(*N*-Cbz)]-OMe (20%); entry 21 in Table 1, *N*-Fmoc-Lys(*N*-Cbz)-Ser[*N*-Fmoc-Lys(*N*-Cbz)]-NH2 (20%) (Supplementary Figure 6).

The great utility of the mechanochemical approach is somewhat diminished by the need of a milling device specifically designed for mechanosynthesis [8,18,19]. In this respect, we appraised the opportunity that the peculiar nanometric structure of HAp might consent to conduct the reaction using common laboratory equipment. With this purpose, we performed the coupling between *N*-Boc-Phe-OH and H-Gly-OEt・HCl (0.23 mmol each) in the presence of EDC・HCl*/*HOBt (0.25 mmol each), and HAp (50 mg), in a 100 ml two-necked glass round bottom flask equipped with a standard olive-shaped polytetrafluoroethylene (PTFE)-coated stirring bar (*l* = 3.0 cm), under inert atmosphere. The gently grinded mixture maintained a powdery appearance throughout the reaction process, and after 2 h the expected dipeptide **3c** was obtained in modest amount (39%), albeit in fairly good purity (85%) after the usual work-up (33% net yield). Increased reaction time had little impact on the yield (not shown), while conventional heating at 50◦C led to a modest increase in the recovered peptide (45% crude mixture, 38% net yield; Table 2, entry 1).

Minimal-LAG

To increase the homogeneity of the mixture, the reaction was repeated in the presence of a minimal amount (80–200 μl) of a liquid additive (Table 2, entries 2–6), in other words, the green solvents EtOAc, *t*BuOAc and γ-valerolactone (GVL) [9,10,25]. *N*,*N*'-dimethylpropylene urea (DMPU) and DMSO were also tested; even though these latter are not included among the prominent green solvents, DMPU and DMSO are regarded as acceptable greener alternatives for hazardous dipolar aprotics [8–10,47].

After 2 h, the reaction was quenched and HAp was recovered according to the work-up procedure described previously. While EtOAc and*t*BuOAc gave hardly satisfactory results (entries 2 and 3 in Table 2), the use of 80 μl of DMSO (entry 4) or 100 μl DMPU (entry 5) gave the desired dipeptide in pretty good quantity (crude: 92 and 86%, respectively) and purities (94 and 90%).

Table 2. Minimal solvent-assisted synthesis of peptides 3 from amino acids 1 and amino ester/amide HCl salts 2 (0.23 mmol each), after 2 h at room temperature, in the presence of *N*-ethyl-*N*′-(3-dimethylaminopropyl)carbodiimide-HCl/hydroxybenzotriazole (0.25 mmol each) and hydroxyapatite (50 mg), in a round bottom flask equipped with a polytetrafluoroethylene-coated magnetic stirring bar.

Entry	1	2-HCl	Solvent	Vol (ml)	3	Recovered crude mixture (%)†	Purity (%)†,‡	Yield (%)§
1	Boc-Phe-OH	H-Gly-OEt	–	–	c	45¶	85	38
2	Boc-Phe-OH	H-Gly-OEt	EtOAc	200	c	48	78	37
3	Boc-Phe-OH	H-Gly-OEt	tBuOAc	100	c	52	80	42
4	Boc-Phe-OH	H-Gly-OEt	DMSO	80	c	92	94	86
5	Boc-Phe-OH	H-Gly-OEt	DMPU	100	c	86	90	77
6	Boc-Phe-OH	H-Gly-OEt	GVL	100	c	89	64	57
7	Boc-Phe-OH	H-Gly-NH_2	GVL	100	e	88	84	74
8	Boc-Phe-OH	H-D-Val-OMe	DMSO	80	d	91	96	87
9	Boc-Trp-OH	H-Phe-NH_2	DMSO	80	h	93	95	88
10	Boc-Trp-OH	H-Phe-NH_2	DMSO	80	h	86#	92#	79
11	Fmoc-Lys(Cbz)-OH	H-Ser-NH_2	DMSO	80	q	70††,‡‡	91††,‡‡	64

†Determined after aqueous workup.
‡Determined by RP-HPLC.
§Calculated as the recovered crude mixture x purity (%).
¶Conducted at 50◦C.
#With HAp (48 mg) recovered from the preceding entry.
††After filtration through a pad of silica gel.
‡‡The depsitripeptide was detected only in traces of (_5%) by RP-HPLC and ESI-MS.
Boc: Tert-butyloxycarbonyl; Cbz: Benzyloxycarbonyl; DMPU: *N,N*′-dimethylpropylene urea; DMSO: Dimethyl sulfoxide; ESI-MS: Electrospray ionisation mass spectrometry; Fmoc:
Fluorenylmethyloxycarbonyl; GVL: _-valerolactone; HAp: Hydroxyapatite; RP-HPLC: Reverse phase high-performance liquid chromatography.

To our surprise, the reaction in GVL (entry 6) gave the expected *N*-Boc-Phe-Gly-OEt dipeptide (**3c**) in low purity (64%). As it turned out, the reaction mixture presented significant amounts of various oligomers at the *N*-terminus, tripeptide *N*-Boc-Phe-Phe-Gly-OEt (18%) and tetrapeptide *N*-Boc-Phe-Phe-Phe-Gly-OEt (5%), as revealed by RP-HPLC/ESI-MS analysis (Supplementary Figure 7). Possibly, these by-products are the consequence
of partial removal of the acid-labile *N*-Boc protecting group. Lewis and Brønsted acid sites coexist with basic sites
on the surface of HAp [38,40]. A recent study on the HAp-catalyzed transformation of ethanol to *n*-butanol revealed
the key role played by the cooperation between the acid and basic sites, and the importance of the simultaneous presence of two weak acid-base pairs, namely Ca2+-OH- and POH-OH-, on the catalytic properties of HAp [39]. On the other hand, the reaction between *N*-Boc-Phe-OH and H-Gly-NH2 in GVL (entry 7 in Table 2) gave the expected *N*-Boc-Phe-Gly-NH2 protected dipeptide (**3e**) with better purity (84%), being the unwanted oligomer *N*-Boc-Phe-Phe-Gly-NH2 a side product (<5%) (Supplementary Figure 8).

The efficacy of using DMSO as solvent was confirmed by reacting *N*-Boc-Phe-OH with H-D-Val-OMe · HCl (entry 8), and *N*-Boc-Trp-OH with H-Phe-NH2 · HCl under the same conditions (Table 2, entry 9). As it turned out, these reactions afforded better yields of **3h** (crude reaction mixtures: 91 and 93%, respectively) and purity (>95%) when compared with solvent-free reaction conditions (compare Table 2 and Table 1). As it was the case in the solvent-free protocol, the HAp powder recovered after the work-up from the reaction corresponding to entry 9 in Table 2 proceeded with little loss of efficiency, when reused to promote the reaction between the same,
fresh reagents (compare with entry 10 in Table 2). Finally, the reaction between *N*-Fmoc-Lys(*N*-Cbz)-OH and

H-Ser-NH2 (Table 2, entry 11) proceeded with slightly higher efficiency (70% of crude peptide) with respect to the

solvent-free variant (entry 21 in Table 1). Nevertheless, the desired dipeptide **3q** was obtained with much higher purity (91%). The analysis of the reaction mixture by RP-HPLC and ESI-MS showed only traces (<5%) of the depsitripeptide *N*-Fmoc-Lys(*N*-Cbz)-D-Ser[*N*-Fmoc-Lys(*N*-Cbz)]-OMe (Supplementary Figure 9).

The optimized reaction conditions in the previous section are in line with the principles of green chemistry. Waste prevention is the main focus of our methodology. Atom economy: Compared with SPPS, for which a 3–4 equivalents excess of reagents is advisable, our protocol utilizes a circa 1:1 ratio between all reactants, and reaction

yields are in several cases almost quantitative. Hence, most of the mass of the reactants atoms are incorporated in

the desired peptides. Less hazardous chemical syntheses: The reagents utilized are the distinct amino acids, which

are in general totally safe. The mechanochemistry approach consents to avoid or to strongly limit the volumes of organic solvents. Designing safer chemicals: Intrinsically, bioactive peptides show much less toxicity as compared

with nonpeptide drugs. We have introduced the unprecedented use of HAp as a totally biocompatible inorganic base to replace harmful organic bases. Safer solvents and auxiliaries: The reactions are conducted under solvent-free

or minimal-solvent conditions. In the latter case, good results have been obtained with DMPU and DMSO; albeit having a yellow coding meaning 'usable with some concerns', these aprotic polar solvents have been proposed as greener alternatives to the red coded hazardous DMF [9–11]. The work-up procedures utilize only the green solvents ethanol and EtOAc. Design for energy efficiency: The mechanochemistry approach consents to conduct reactions at ambient temperature and pressure. The limitation of the volume of solvents also allows a significant reduction of the energy consumption in the process. Use of renewable feedstocks: The only solvents utilized in gram scale in our protocol are the green solvents EtOH and EtOAc [9–11,48]. Bioethanol can be produced from sugarcane, molasses, sugar beets, corn kernels, wheat, cassava and sweet potatoes. The main method to manufacture

EtOAc involves the esterification of ethanol with acetic acid. In turn, acetic acid can be conveniently prepared by aerobic fermentation of ethanol. As for DMSO, it can be made by oxidizing the dimethyl sulphide by-product of wood pulping operations. Reduce derivatives: Traditionally, the chemical synthesis of peptides requires repetitive

protection/deprotection steps. In this regard, our protocol has been optimized for using the Boc protecting group (MW = 100 gmol-1) rather than the bulky Fmoc (MW = 222 gmol-1); Boc group is cleaved with gaseous HCl,

and the cleavage by-products are tert-butanol and CO2. Catalysis: This is a fundamental issue of our methodology;

HAp has been reutilized for up to five reaction cycles with little loss of efficacy. Design for degradation: This is a major advantage in the use of bioactive peptides as drugs, compared with small-molecule drugs: at the end of their function, peptides are metabolized into innocuous products and do not persist in the environment. Real-time

analysis for pollution prevention: Traditional mechanochemistry devices such as mills or grinders consent limited

real-time, in-process monitoring and control. In this regard, our reactions can be conducted also into normal

laboratory reactors, making the connection to any sensors much easier. Inherently safer chemistry for accident prevention: There are several aspects in our protocol to intrinsically reduce risks. The reactor operates under very mild conditions (rt, ambient pressure, low-speed milling, etc.), making the risk of accidental release very limited. The process needs no excess of any reagents; most of reagents are nontoxic, the base HAp is fully biocompatible; reaction solvents are absent or are utilized in microliter scale; the bulky solvents are in the green solvents list. Hence, even in case of accidental release the mixture could safely be disposed-off.

Solvent-free synthesis of H-Tyr-Pro-Trp-Phe-NH2 (endomorphin-1)

We exploited the solvent-free protocol for the preparation of a relevant bioactive peptide. As a continuation of our efforts in the area of opioid peptides [49–52], we opted for the tetrapeptide endomorphin-1 (EM1), H-Tyr-Pro-Trp-Phe-NH2, the endogenous ligand of the μ-opioid receptor [53], currently regarded as a fundamental lead for the design of painkillers devoid of harmful side effects. Previously, EM1 was synthesized under green chemistry conditions by a combination of enzymatic and chemical methods. Peptide Boc-Trp-Phe-NH2 was synthesized in a 20% methanol medium using the protease WQ9-2, while Boc-Tyr-Pro-OH was synthesized chemically. The tetrapeptide was obtained in good yield by the protease PT121 in an organic-aqueous biphasic system [54]. EM1 was also obtained with acceptable yield and purity in aqueous conditions by SPPS on a polyethylene glycol (PEG)-based ChemMatrix peptide amide resin, using *N*-carboxyanhydrides as activated/protected derivatives of the amino acids, without the need of coupling reagents nor protecting groups [13].

The dipeptide *N*-Boc-Trp-Phe-NH2 (**3h**, Table 1, entry 14) was treated with gaseous HCl for the removal of the *N*-Boc protecting group [25], to quantitatively yield the salt H-Trp-Phe-NH2 · HCl (**4**), which was coupled to Boc-Pro-OH (Figure 4). After the usual work-up, the crude tripeptide *N*-Boc-Pro-Trp-Phe-NH2 (**5**) was obtained in satisfactory amount (65%) and chromatographic purity (77%). The removal of *N*-Boc protecting group as before, and subsequent coupling with *N*-Boc-Tyr-OH, afforded *N*-Boc-protected EM1 (**5**, Figure 4) in reasonable amount (68%) and purity (89%; Supplementary Figure 10). After Boc deprotection, to remove the residual organic impurities, the resulting tetrapeptide salt **7** was suspended in EtOAc and sonicated; EM1 · HCl was collected by centrifuge in almost quantitative yield and excellent purity (94%; Supplementary Figure 11).

Conclusion

In this paper, we report the unprecedented use of nanocrystalline HAp powder to promote the reaction between *N*-protected amino acids and a variety of amino · HCl partners, in the presence of the coupling agentsEDC · HCl/HOBt.

The peculiar structure of HAp allowed smooth mechanochemical solvent-free condensation reactions under mild

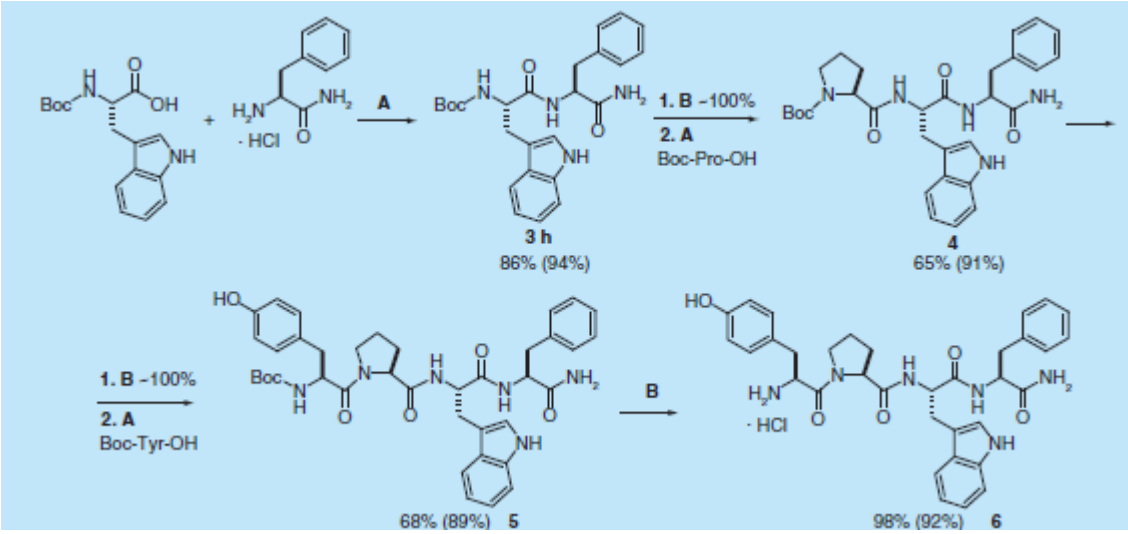

Figure 4. Solvent-free synthesis of endomorphin-1. Reagents and conditions: **(A)** HOBt (1.2 eq), EDC (1.2 eq), HAp (50 mg), rt, 2 h. **(B)** Gaseous HCl, rt, 3 h. The percentages refer to the amount of crude peptides recovered after standard aqueous work-up; chromatographic (RP-HPLC) purities (%) are reported in brackets. Boc: Tert-butyloxycarbonyl; EDC: *N*-ethyl-*N*_-(3-dimethylaminopropyl)carbodiimide; ESI-MS: Electrospray ionisation mass spectrometry; HAp: Hydroxyapatite; HOBt: HCl/hydroxybenzotriazole; RP-HPLC: Reverse phase high-performance liquid chromatography; rt: Room temperature.

conditions, as well as minimal solvent-assisted reactions conducted in common laboratory glassware. Compared with pre-existing methods based on inorganic bases [18,19,25,27], our protocol utilizes a totally biocompatible material.

Furthermore, the mineral powder can be reutilized for several cycles with little loss in efficiency. Plausibly, HAp acts as a sort of chemical sponge capable to passively absorb anhydrous HCl into its open channels, leaving the crystalline structure intact, as confirmed by the comparison of the x-ray analyses of fresh and recycled powders.

Future perspective

To substantiate the practical efficacy of HAp, we were able to obtain the native opioid tetrapeptide EM1 by solventfree

ball-milling in satisfactory yield and purity. In perspective, the method can find application to the synthesis of a variety of bioactive oligopeptides under environmentally benign conditions. This gratifying result contributes to

assert the green transition also in the field of peptide application programming interfaces.

Summary points

- Synthetic stoichiometric nanocrystalline hydroxyapatite (HAp) is a fully biocompatible calcium phosphate mineral with similar composition to bone-forming apatites.
- HAp nano powder was positively tested as inorganic base to foster peptide bond formation by 'dry' ball-milling.
- Excellent results were obtained under minimally 'wet' conditions with *N*,*N*'-dimethylpropylene urea or dimethyl sulfoxide, acceptable greener alternatives for hazardous dipolar aprotic solvents.
- Compared with Boc, Fmoc protecting group gave inferior yields; besides, the unreacted Fmoc-amino acids were recovered much less efficiently by basic water extraction of the crude reaction mixtures.
- Solvent-free reactions of hydroxy-unprotected serine gave some depsipeptides, while under minimal solvent grinding conditions the depsipeptides were observed in traces.
- Thanks to the peculiar crystal structure, HAp acts as an HCl sponge, which can be reused for several cycles.

• The proposed protocol meets the requisites of green chemistry.

• The use of HAp allowed the expedient green preparation of endomorphin-1, the endogenous ligand of μ-opioid receptor.

Supplementary data

To view the supplementary data that accompany this paper please visit the journal website at: www.future-science.com/doi/suppl/10.4155/fmc-2019-0320

Financial & competing interests disclosure

The authors thank the Fondazione del Monte di Bologna e Ravenna for financial support (Proj. "IntegrAL" n◦ 328bis/2017). The authors have no other relevant affiliations or financial involvement with any organization or entity with a financial interest in or financial conflict with the subject matter or materials discussed in the manuscript apart from those disclosed.

No writing assistance was utilized in the production of this manuscript.

References

Papers of special note have been highlighted as: · of interest; ·· of considerable interest

1. Gentilucci L, Tolomelli A, Squassabia F. Peptides and peptidomimetics in medicine, surgery and biotechnology. *Curr. Med. Chem.* 13(20), 2449–2466 (2006).

2. Henninot A, Collins JC, Nuss JM. The current state of peptide drug discovery: back to the future? *J. Med. Chem.*

61(4), 1382–1414 (2018).

3. Gentilucci L, De Marco R, Cerisoli L. Chemical modifications designed to improve peptide stability: incorporation of non-natural amino acids, pseudo-peptide bonds, and cyclization. *Curr. Pharm. Des.* 16(28), 3185–3203 (2010).

4. Zompra AA, Galanis AS, Werbitzky O, Albericio F. Manufacturing peptides as active pharmaceutical ingredients. *Future Med. Chem.* 1(2), 361–377 (2009).

5. Gentilucci L, Tosi P, Bauer A, De Marco R. Modern tools for the chemical ligation and synthesis of modified peptides and proteins. *Future Med. Chem.* 8(18), 2287–2304 (2016).

6. Jad YE, Kumar A, El-Faham A, de la Torre BG, Albericio F. Green transformation of solid-phase peptide synthesis. *ACS Sustain. Chem.Eng.* 7(4), 3671–3683 (2019).

·· A comprehensive review on recent green techniques, reagents, solvents, for solid phase and liquid peptide synthesis.

7. Isidro-Llobet A, Kenworthy MN, Mukherjee S *et al.* Sustainability challenges in peptide synthesis and purification: from R&D to production. *J. Org. Chem.* 84(8), 4615–4628 (2019).

8. Varnava KG, Sarojini V. Making solid-phase peptide synthesis greener: a review of the literature. *Chem. Asian J.*

14(8), 1088–1097 (2019).

9. Prat D, Hayler J, Wells A. A survey of solvent selection guides. *Green Chem.* 16(10), 4546–4551 (2014).

10. Prat D, Wells A, Hayler J *et al*. CHEM21 selection guide of classical and less classical-solvents. *Green Chem.* 18(1), 288–296 (2016).

·· A methodology based on safety, health and environment criteria enables a greenness evaluation of bio-derived solvents.

11. Byrne FP, Jin S, Paggiola G *et al.* Tools and techniques for solvent selection: green solvent selection guides. *Sustain. Chem. Process* 4(7), doi:10.1186/s40508-016-0051-z (2016).

12. Hojo K, Shinozaki N, Nozawa Y, Fukumori Y, Ichikawa H. Aqueous microwave-assisted solid-phase synthesis using Boc-amino acid nanoparticles. *Appl. Sci.* 3(3), 614–623 (2013).

13. De Marco R, Tolomelli A, Greco A, Gentilucci L. Controlled solid phase peptide bond formation using *N*-carboxyanhydrides and PEG resins in water. *ACS Sustain. Chem. Eng.* 1(6), 566–569 (2013).

·· Solid-phase synthesis of peptides is conducted in aqueous medium with excellent atom economy, without the need of protecting groups nor activating agents.

14. Cortes-Clerget M, Berthon J-Y, Krolikiewicz-Renimel I, Chaisemartin L, Lipshutz BH. Tandem deprotection/coupling for peptide synthesis in water at room temperature. *Green Chem.* 19(18), 4263–4267 (2017).

15. Galanis AS, Albericio F, Grotli M. Solid-phase peptide synthesis in water using microwave-assisted heating. *Org. Lett.*11(20), 4488–4491 (2009).

· A method for the solid-phase synthesis of peptides using the most common Boc-amino acid derivatives was developed, using polyethylene glycol (PEG)-based resin, *N*-ethyl-*N*_-(3-dimethylaminopropyl)carbodiimide-HONB as a coupling method, and microwave (MW) irradiation as an energy source.

16. Castaldo M, Barlind L, Mauritzson F, Wan PT, Snijder HJ. A fast and easy strategy for protein purification using “teabags”. *Sci. Rep.* 6, 28887 (2016).

17. Volkmer R. Synthesis and application of peptide arrays: quo vadis SPOT technology. *ChemBioChem* 10(9), 1431–1442 (2009).

18. Declerck V, Nun P, Martinez J, Lamaty F. Solvent-free synthesis of peptides. *Angew. Chem. Int. Ed.* 48(49), 9318–9321 (2009).

·· Here is reported a straightforward, high-yielding method for the preparation of peptides with no epimerization and in the absence of solvent, involving the reaction of Boc-*N*-carboxyanhydrides.

19. Landeros JM, Juaristi E. Mechanochemical synthesis of dipeptides using Mg–Al hydrotalcite as activating agent under solvent-free reaction conditions. *Eur. J. Org. Chem.* 2017(3), 687–694 (2017).

·· Mg–Al hydrotalcite minerals as green activating agent offered several advantages: the use of readily available reagents and inexpensive materials, easy workup, simple recovery and recyclability, and short reaction times.

20. Gonnet L, Tintillier T, Venturini N *et al. N*-Acyl benzotriazole derivatives for the synthesis of dipeptides and tripeptides and peptide biotinylation by mechanochemistry. *ACS Sustain. Chem. Eng.* 5(4), 2936–2941 (2017).

21. Hern´andez JG, Juaristi E. Green synthesis of α,β- and β,β-dipeptides under solvent-free conditions. *J. Org. Chem.*

75(21), 7107–7111 (2010).

·· *N*-Boc-*N*-carboxyanhydrides were employed under ball-milling activation, giving α,β- and β,β-dipeptides.

22. Maurin O, Verdi´e P, Subra G *et al.* Peptide synthesis: ball-milling, in solution, or on solid support, what is the best strategy? *Beilstein J. Org. Chem.* 13, 2087–2093 (2017).

23. Hern´andez JV, Ardila-Fierro KJ, Crawford D, James SL, Bolm C. Mechanoenzymatic peptide and amide bond formation. *Green Chem.* 19(11), 2620–2625 (2017).

·· Mechanochemical chemoenzymatic peptide and amide bond formation catalyzed by papain was studied by ball milling.

24. Ardila-Fierro KJ, Crawford DE, K¨orner A, James SL, Bolm C, Hern´andez JG. Papain-catalysed mechanochemical synthesis of oligopeptides by milling and twin-screw extrusion: application in the Juli´a-Colonna enantioselective epoxidation. *Green Chem.* 20(6), 1262–1269 (2018).

25. Bonnamour J, Metro T-X, Martinez J, Lamaty F. Environmentally benign peptide synthesis using liquid-assisted ball milling: application to the synthesis of Leu-enkephalin. *Green Chem.* 15(5), 1116–1120 (2013).

· An original methodology for peptide bond synthesis avoiding toxic solvents and reactants was successfully applied to the synthesis of Leu-enkephalin.

26. Porte V, Thioloy M, Pigoux T, Metro T-X, Martinez J, Lamaty F. Peptide mechanosynthesis by direct coupling of N-protected α-amino acids with amino esters. *Eur. J. Org. Chem.* 2016(21), 3505–3508 (2016).

27. Morales-Serna JA, Jaime-Vasconcelos MA, Garc´ıa-R´ıos E, Cruz A *et al.* Efficient activity of magnesium–aluminium hydrotalcite in the synthesis of amides. *RSC Adv.* 3(45), 23046–23050 (2013).

28. Bigi A, Boanini E. Functionalized biomimetic calcium phosphates for bone tissue repair. *J. Appl. Biomater. Funct. Mater.* 15(4), e313–e325 (2017).

29. Boanini E, Cassani MC, Rubini K, Boga C, Bigi A. (9R)-9-Hydroxystearate-functionalized anticancer ceramics promote loading of silver nanoparticles. *Nanomaterials* 8(6), E390 (2018).

30. Zhu Y-J, Lu B-Q. Deformable biomaterials based on ultralong hydroxyapatite nanowires. *ACS Biomater. Sci.* 5(10), 4951–4961 (2019).

31. Haider A, Haider S, Hanb SS, Kang I-K. Recent advances in the synthesis, functionalization and biomedical applications of hydroxyapatite: a review. *RSC Adv.* 7(13), 7442–7458 (2017).

32. Ng H-M, Bee S-T, Tin Sin L, Ratnam CT, Rahmat AR. Hydroxyapatite for poly(α-hydroxy esters) biocomposites applications. *Polym. Rev.* 59(2), 187–239 (2019).

33. Wei G, Gong C, Hu K, Wang Y, Zhang Y. Biomimetic hydroxyapatite on graphene supports for biomedical applications: a review. *Nanomaterials* 9(10), 1435 (2019)

34. Gomes DS, Santos AMC, Neves GA, Menezes RR. A brief review on hydroxyapatite production and use in biomedicine. *Ceramica* 65, 282–302 (2019).

35. Neacsu IA, Stoica AE, Vasile BS, Andronescu E. Luminescent hydroxyapatite doped with rare earth elements for biomedical applications. *Nanomaterials* 9(2), 239 (2019).

36. Fihri A, Len C, Varma RS, Solhy A. Hydroxyapatite: a review of syntheses, structure and applications in heterogeneous catalysis. *Coord. Chem. Rev.* 347, 48–76 (2017).

· The significant applications of hydroxyapatite both as an inorganic support and as a catalyst are described with an emphasis on its performance, stability and reusability.

37. Kaneda K, Mizugaki T. Design of high-performance heterogeneous catalysts using apatite compounds for liquid-phase organic syntheses. *ACS Catalysis* 7(2), 920–935 (2017).

38. Ben Osman M, Diallo Garcia S, Krafft J-M *et al*. Control of calcium accessibility over hydroxyapatite by post-precipitation steps: influence on the catalytic reactivity toward alcohols. *Phys. Chem. Chem. Phys.* 18(40), 27837–27847 (2016).

39. Ben Osman M, Krafft J-M, Thomas C, Yoshioka T, Kubo J, Costentin G. Importance of the nature of the active acid/base pairs of hydroxyapatite involved in the catalytic transformation of ethanol to n-butanol revealed by operando DRIFTS. *ChemCatChem* 11(6), 1765–1778 (2019).

40. Diallo-Garcia S, Ben Osman M, Krafft JM *et al*. Identification of surface basic sites and acid-base pairs of hydroxyapatite. *J. Phys. Chem. C* 118(24), 12744–12757 (2014).

41. Tavafoghi M, Cerruti M. The role of amino acids in hydroxyapatite mineralization. *J. R. Soc. Interface* 13(123), 20160462 (2016).

42. Wro´oblewska A, Paluch P, Wielgus E, Bujacz G, Dudek MK, Potrzebowski MJ. Approach toward the understanding of coupling mechanism for EDC reagent in solvent-free mechanosynthesis. *Org. Lett.* 19(19), 5360–5363 (2017).

· Solid-state nuclear magnetic resonance, x-ray crystallography and theoretical calculations are employed to study the mechanism of the formation of the C–N amide bond using *N*-ethyl-*N*_-(3-dimethylaminopropyl) carbodiimide · HCl.

43. Bigi A, Boanini E, Gazzano M, Kojdeckic MA, Rubini K. Microstructural investigation of hydroxyapatite–polyelectrolyte composites. *J. Mater. Chem.* 14(2), 274–279 (2004).

44. Mekhemer GAH, Bongard H, Shahin AAB, Zaki MI. FTIR and electron microscopy observed consequences of HCl and CO2 interfacial interactions with synthetic and biological apatites: influence of hydroxyapatite maturity. *Mater. Chem Phys.* 221, 332–341 (2019).

45. Nguyen TV, Lyons DJM. A novel aromatic carbocation-based coupling reagent for esterification and amidation reactions. *Chem. Commun.* 51(15), 3131–3134 (2015).

46. Zaki MI, Kn¨ozinger H, Tesche B. Structural and morphological consequences of high-temperature treatments of hydroxyapatite in the absence or presence of HCl vapor. *Langmuir* 22(2), 749–755 (2006).

47. Pawlas J, Rasmussen JH. ReGreen SPPS: enabling circular chemistry in environmentally sensible solid-phase peptide synthesis. *Green Chem.* 21(21), 5990–5998 (2019).

48. Jad YE, Acosta GA, Govender T *et al.* Green solid-phase peptide synthesis 2. 2-Methyltetrahydrofuran and ethyl acetate for solid-phase peptide synthesis under green conditions. *ACS Sustain. Chem. Eng.* 4, 6809–6814 (2016).

· Green solvents, temperature, solid supports and peptide models were evaluated in this study to establish the best green protocol.

49. Adamska-Bart-lomiejczyk A, De Marco R, Gentilucci L, Kluczyk A, Janecka A. Design and characterization of opioid ligands based on cycle-in-macrocycle scaffold. *Bioorg. Med. Chem.* 25(8), 2399–2405 (2017).

50. De Marco R, Gentilucci L. Tryptophan-containing non-cationizable opioid peptides – a new chemotype with unusual structure and *in vivo* activity. *Future Med. Chem.* 9(17), 2099–2115 (2017).

51. Wtorek K, Artali R, Piekielna-Ciesielska J *et al.* Endomorphin-2 analogs containing modified tyrosines: biological and theoretical investigation of the influence on conformation and pharmacological profile. *Eur. J. Med. Chem.* 179, 527–536 (2019).

52. DeMarco R, Bedini A, Spampinato S *et al.* Constraining endomorphin-1 by β,α-hybrid dipeptide/heterocycle scaffolds: identification of a novel κ-opioid receptor selective partial agonist. *J. Med. Chem.* 61(13), 5751–5757 (2018).

·· The modification of the mu-opioid receptor agonist edomorphin-1 resulted in a new chemotype of selective, partial KOR agonist inducing analgesia, therefore displaying great potential interest as a painkiller possibly with reduced harmful side effects.

53. Zadina JE, Hackler L, Ge LJ, Kastin AJ. A potent and selective endogenous agonist for the mu-opiate receptor. *Nature* 386(6624), 499–502 (1997).

·· The tetrapeptides edomorphin-1 and -2 were identified in mammalian and were recognized to be endogenous agonists for the mu opioid receptor.

54. Sun H, He B, Xu J, Wu B, Ouyang P. Efficient chemo-enzymatic synthesis of endomorphin-1 using organic solvent stable proteases to green the synthesis of the peptide. *Green Chem.* 13(7), 1680–1685 (2011).

· The chemo-enzymatic synthesis of edomorphin-1 proved to be productive, with minimal side-chain protection and simple purification, thus validating the chemo-enzymatic approach for peptide synthesis.